ORIGINAL RESEARCH

MR Imaging Criteria for the Prediction of Extranodal Spread of Metastatic Cancer in the Neck

Y. Kimura
M. Sumi
N. Sakihama
F. Tanaka
H. Takahashi
T. Nakamura

BACKGROUND AND PURPOSE: The presence of extranodal spread in metastatic nodes significantly affects treatment planning and prognosis of the patient with head and neck cancer. We attempted to evaluate the predictive capability of MR imaging for the extranodal spread in the neck.

MATERIALS AND METHODS: We retrospectively studied MR images from 109 patients with histologically proved metastatic nodes, of which 39 were positive for extranodal spread. We assessed 47 extranodal spread–positive and 130 extranodal spread–negative metastatic nodes by using the following MR imaging findings as the possible criteria for extranodal spread: 1) nodal size (short-axis diameter); 2) obliterated fat spaces between the metastatic node and adjacent tissues, such as the muscles and skin on T1-weighted images ("vanishing border" sign); 3) the presence of high-intensity signals in the interstitial tissues around and extending from a metastatic node on fat-suppressed T2-weighted images ("flare" sign); and 4) an irregular nodal margin on gadolinium-enhanced T1-weighted images ("shaggy margin"). Multivariate logistic regression analysis was conducted to identify independent predictive criteria for extranodal spread.

RESULTS: Nodal size, shaggy margin, and flare sign criteria were independent and significant MR imaging findings suggestive of extranodal spread in the metastatic nodes. We obtained 77% sensitivity and 93% specificity with the flare sign, 65% sensitivity and 99% specificity with the shaggy margin, and 80% sensitivity and 85% specificity with the size criterion (cutoff point = 16 mm).

CONCLUSION: Fat-suppressed T2-weighted and gadolinium-enhanced T1-weighted images are useful for the detection of extranodal spread in metastatic nodes in the neck.

Locoregional recurrence and the development of second primary tumors after surgical resection is a major problem in head and neck cancer management.[1] Extranodal spread (ENS) is one of the high-risk features in patients with head and neck cancer because the presence of ENS is associated with an increase in the incidence of locoregional recurrence and distant metastasis.[2-4]

CT and MR imaging are frequently used to stage cancer, and CT has been shown to be more accurate than MR imaging.[5] Recent studies suggested some improvement of the MR imaging technique in the diagnosis of metastatic nodes in the neck.[6,7] Along with this progress, a recent study comparing CT and MR imaging showed that CT and MR imaging are comparable for the detection of ENS in the neck.[8] Compared with other imaging characteristics of metastatic nodes, such as nodal necrosis, ENS is much more difficult to assess by CT and MR imaging, due to the lack of definite imaging criteria for ENS. In general, ENS is defined on CT and MR images as a metastatic node with indistinct nodal margins, irregular nodal capsular enhancement, and infiltration into the adjacent fat or muscle.[8]

We reasoned that MR imaging with recently improved techniques could more readily detect changes characteristic of ENS in the neck. To test this hypothesis, we retrospectively assessed potential MR imaging findings suggestive of ENS in patients with ENS in the necks.

Received June 29, 2006; accepted after revision February 6, 2008.

From the Department of Radiology and Cancer Biology (Y.K., M.S., T.N.), Nagasaki University School of Dentistry, Nagasaki, Japan; and Department of Otolaryngology (N.S., F.T., H.T.), Nagasaki University School of Medicine, Nagasaki, Japan.

Please address correspondence to Takashi Nakamura, DDS, PhD, Department of Radiology and Cancer Biology, Nagasaki University School of Dentistry, 1-7-1 Sakamoto, Nagasaki 852-8588, Japan; e-mail: taku@nagasaki-u.ac.jp

DOI 10.3174/ajnr.A1088

Materials and Methods

Subjects

We evaluated the MR images of 116 patients with head and neck cancers, who had undergone MR examinations for staging of nodal metastasis from 2002 to 2006. Of these patients, 7 were excluded from the study due to significant motion artifacts in the MR images, leaving images from 109 patients (20 women and 89 men; average age, 66 ± 10 years) with histologically proved metastatic nodes in the neck. The study cohort included patients with cancers in the tongue ($n = 33$), hypopharynx ($n = 13$), oropharynx ($n = 12$), lower gingiva ($n = 9$), upper gingiva ($n = 7$), thyroid ($n = 6$), maxillary sinus ($n = 5$), parotid gland ($n = 4$), submandibular gland ($n = 3$), nasopharynx ($n = 3$), palate ($n = 3$), larynx ($n = 3$), nasal cavity ($n = 2$), and unknown ($n = 6$). Histologic types were squamous cell carcinomas ($n = 95$), papillary carcinomas ($n = 6$), mucoepidermoid carcinomas ($n = 3$), adenoid cystic carcinomas ($n = 2$), adenocarcinomas ($n = 2$), and carcinoma ex pleomorphic adenoma ($n = 1$).

Surgical impression at neck dissection and subsequent histologic examinations confirmed that 39 (7 women and 32 men) of the 109 patients had 1 or more metastatic nodes with ENS. Thus, we analyzed 47 ENS-positive and 130 ENS-negative metastatic nodes in the necks of the 109 patients. Pathologists and surgeons (otolaryngologists) reviewed the thin sections (microscopic ENS) or bivalve sections (macroscopic ENS) or both of all nodes suggestive of ENS. ENS-positive nodes were defined as those with macroscopic or microscopic cancer spreads beyond the nodal capsules.

Table 1: Incidence (%) of MR imaging findings in the necks of patients with head and neck cancers by consensus of 2 radiologists

	Vanishing Border Sign* (T1WI)		Flare Sign* (fsT2WI)		Shaggy Margin* (CET1WI)	
	Present	Absent	Present	Absent	Present	Absent
ENS (+)	91	6	90	7	97	0
ENS (−)	10	33	8	35	12	31
Total	101	39	98	42	109	31

Note:—T1WI indicates T1-weighted imaging; fT2WI, fat-suppressed T2-weighted imaging; CET1WI, gadolinium-enhanced T1-weighted imaging.
* The incidence of MR imaging criteria is significantly different between ENS (+) and ENS (−) necks ($P < .0001$, Fisher exact test).

MR Imaging

MR imaging was performed by using a 1.5T MR imager (Gyroscan Intera 1.5T Master; Philips Medical System, Best, Netherlands) with a head and neck coil (Synergy Head Neck Coil; Philips Medical Systems) or a surface coil (Synergy Flex L Coil, 22 cm; Philips Medical Systems). Axial and coronal T1-weighted images (TR/TE = 500/15 ms; number of signal-intensity acquisitions, 4) and axial fat-suppressed spectral presaturation with inversion recovery (SPIR) T2-weighted images (TR/TE = 4674/80 ms; number of signal-intensity acquisitions, 4) were obtained from all the patients by using a conventional spin-echo sequence and a turbo spin-echo sequence, respectively. Gadolinium-enhanced T1-weighted images (TR/TE = 500/15 ms; number of signal-intensity acquisitions, 4) were obtained by using a conventional spin-echo sequence. The section thickness was 4 mm. The MR imaging was performed with a 204 × 256 matrix, a 20-cm FOV, and an 0.4-mm intersection gap. Gadolinium was injected intravenously at a dose of 0.2 mL/kg of body weight.

Correlation of Dissected Lymph Nodes to MR Imaging

We ensured that the node being studied histologically was the same node seen on MR imaging by making a node map for each patient, where MR imaging findings of metastatic nodes with or without ENS and of reactive nodes were illustrated. The map included data concerning the approximate location relative to the surrounding anatomic structures, such as vessels and muscles,[9] and the sizes of the metastatic and reactive nodes on MR images. The metastatic and reactive nodes indicated by MR imaging were numbered by the radiologists. At surgery, nodes were taken out in clusters and the surgeons correlated the excised nodes with those on the map. These procedures enabled the surgeons to correlate the dissected nodes to the nodes evaluated by MR imaging.

Interpretation of MR Images

We evaluated the MR images for the presence or absence of ENS on the basis of the previously reported MR imaging criteria.[8] These criteria included the following: 1) obliterated fat space between the node and adjacent tissues, such as the muscles and skin ("vanishing border" sign); 2) high-intensity signal intensity present in the interstitial tissues located around and extending from the metastatic node ("flare" sign); and 3) irregular or interrupted enhancement at the periphery of the nodes (interrupted nodal rim). These MR imaging criteria were evaluated on T1-weighted and fat-suppressed T2-weighted images (Fig 1) or on gadolinium-enhanced T1-weighted images (Fig 2). The decision regarding MR imaging results was made according to the consensus of 2 readers, blinded to the results, and the results were compared with the histologic results obtained by a fourth observer. The 3 radiologists had 8- and 10-year clinical experience in the field of head and neck MR imaging.

Additionally, the short-axis diameters of nodes were measured by using a caliper on an axial T1-weighted image where the maximum area of a node was seen. Thus, the short axis crosses at a right angle to the longest diameter of the maximal area of the node. The predictive ability of the short-axis diameter for ENS was assessed after varying the cutoff size of the short-axis diameter.

The MR imaging finding of each node with or without ENS was compared on a one-to-one basis with the correlative pathologic findings. This comparison was done by making a node map for each patient, in which MR imaging findings of metastatic nodes with or without ENS and of reactive nodes were noted by radiologists. At surgery, the surgeons correlated the excised nodes with those on the map.

Logistic analysis was performed to identify MR imaging characteristics that could be used as predictive indicators for differentiating metastatic nodes with and without extranodal spread. MR imaging

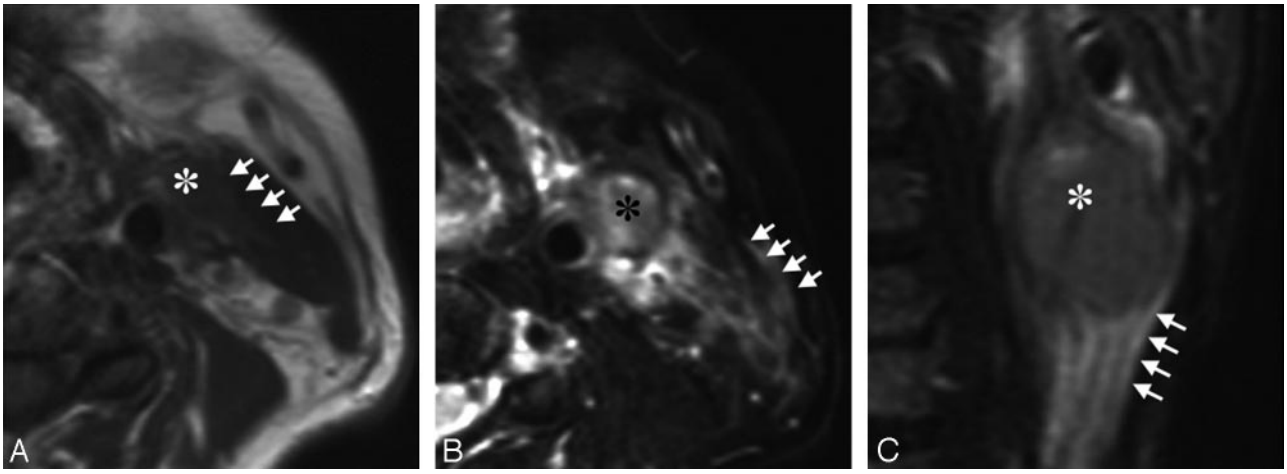

Fig 1. A 63-year-old man with tongue carcinoma. *A,* Axial T1-weighted (TR/TE = 500/15) image shows an ENS-positive metastatic node (*asterisk*) at level II. Note the vanishing border sign (*arrows*) with obliteration of the fat layer between the node and the neighboring sternocleidomastoid muscle. *B,* Axial fat-suppressed T2-weighted (TR/TE = 4674/80 ms) image shows the flare sign that is around and extending from the same ENS-positive metastatic node (*asterisk*) as in *A.* Note that high-intensity signals are present in the interstitial tissues between the sternocleidomastoid muscle and the subcutaneous fat (*arrows*). *C,* Coronal fat-suppressed T2-weighted (TR/TE = 4674/80 ms) image shows the flare sign (*arrows*) caudal to the same ENS-positive metastatic node (*asterisk*) as in *A* and *B.*

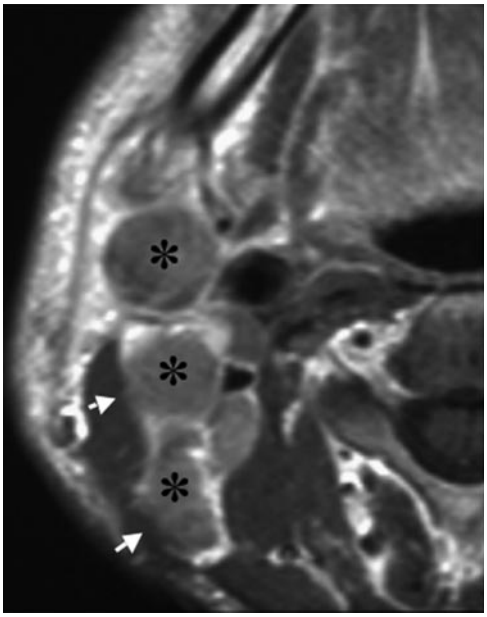

Fig 2. A 51-year-old man with upper gingival carcinoma. Gadolinium-enhanced axial T1-weighted (TR/TE = 500/15) image shows the irregular boundary (shaggy margin, *arrows*) of contrast-enhanced metastatic nodes with ENS (*asterisk*) at levels II and III.

findings that were found to be important in univariate analysis were entered into multivariate models to determine their independent predictive value.[10] Stepwise analysis was performed as a forward stepping procedure based on a likelihood ratio test, with a P value $< .05$ for variable inclusion and $P > .1$ for exclusion from the model. The results were also evaluated by calculating odds ratios. Stepwise logistic regression analysis was performed with the statistical software package Statistical Package for the Social Sciences for Windows, Version 6.1 (SPSS, Chicago, Ill). Diagnostic abilities were evaluated by calculating sensitivity, specificity, accuracy, and positive and negative predictive values for single uses of the independent MR imaging criteria. We also assessed the diagnostic abilities for combinations of 2 or more of these MR imaging criteria; a metastatic node was diagnosed as ENS-positive if it exhibited at least 1 of any combination of the independent MR imaging criteria. Univariate data were evaluated by using a χ^2 test of the logical variables and a Mann-Whitney U test for the size.

Results

MR Imaging Findings of Extranodal Spread

We found that the following MR imaging findings were frequently observed with ENS-positive nodes (Table 1): 1) obliteration of the fat planes between metastatic nodes and adjacent tissues such as the muscles and skin as seen on T1-weighted images (vanishing border sign); 2) high-intensity signal around and extending from a metastatic node, as seen on fat-suppressed T2-weighted images (flare sign); and 3) an irregular modal margin ("shaggy margin") of a node seen on gadolinium-enhanced T1-weighted images (Figs 1 and 2). In addition, the short-axis diameters of ENS-positive metastatic nodes were significantly greater than those of ENS-negative metastatic nodes (Fig 3).

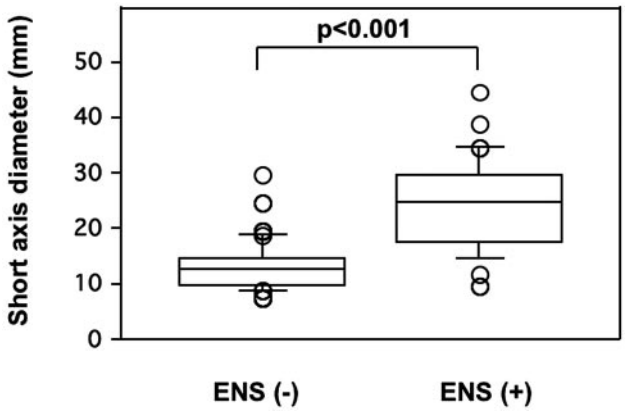

Fig 3. Comparison of nodal sizes of ENS-positive and -negative metastatic nodes in the neck. Graph (boxplots) shows distributions of short-axis diameters of ENS-negative (−) ($n = 130$) and ENS-positive (+) ($n = 47$) metastatic nodes in the necks from 109 patients with head and neck cancers. The horizontal line is a median (50th percentile) of the measured volumes; the tops and bottoms of the boxes represent the 25th and 75th percentiles, respectively, and whiskers indicate the range from the largest to smallest observed data points within the 1.5 interquartile range presented by the box. The short-axis diameters of ENS (+) metastatic nodes are significantly greater than those of ENS (−) metastatic nodes (P value, Mann-Whitney U test).

Table 2: Multivariate analyses of MR imaging findings

Variable	Coefficient	95% CI	SE	Odds Ratio	P
Short-axis diameter	−0.029	−0.045 to −0.016	0.009	6.8	.017*
Vanishing border sign	0.325	0.213 to 0.647	0.258	6.8	.350
Flare sign	−0.773	−0.952 to −0.556	0.325	8.3	.005*
Shaggy margin	−0.334	−0.22 to −0.462	0.274	7.5	<.001*

Note:—CI indicates confidence interval.
* Independent and significant MR imaging findings.

Logistic Regression Analysis of MR Imaging Findings of Extranodal Spread

At univariate analysis, all 4 of the MR imaging findings significantly contributed to the prediction of extranodal spread ($P < .001$). Therefore, these 4 MR imaging criteria were entered into multivariate models to determine their independent predictive value. Multivariate analyses indicated that nodal size and the presence of the flare sign or shaggy margin significantly and independently contributed to the prediction of ENS in the metastatic nodes, but the presence of the vanishing border sign did not (Table 2). The odds ratio indicated that the former 2 MR imaging criteria were both indicative of ENS in the metastatic nodes.

Diagnostic Ability of MR Imaging Findings

Given that the previously mentioned 2 MR imaging criteria were useful for the prediction of ENS, we next assessed the diagnostic ability of these criteria. As shown in Table 3, the flare sign and shaggy margin criteria provided similar levels of accuracy, whereas sensitivity with the shaggy margin was lower than that in the other 2 criteria (flare sign and size). The size criterion (cutoff point = 16 mm) was less predictive. However, any combination of 2 or 3 of the independent MR imaging criteria did not significantly increase the diagnostic abilities of a single use of the flare sign criterion (data not shown).

Table 3: Diagnostic ability of MR imaging criteria for ENS

MR Imaging Findings	Diagnostic Ability (%)				
	Sensitivity	Specificity	Accuracy	PPV	NPV
Flare sign (fsT2WI)	77	93	88	83	90
Shaggy margin (CET1WI)	65	99	89	86	86
Short-axis diameter					
15 mm	93	66	75	61	94
16 mm	80	85	84	76	88
17 mm	78	84	81	74	87

Note:—fsT2WI indicates fat-suppressed T2-weighted imaging; CET1WI, gadolinium-enhanced T1-weighted imaging; PPV, positive predictive value; NPV, negative predictive value.

Discussion

We have assessed the diagnostic ability of various MR imaging criteria for ENS in the necks of patients with head and neck cancer. We found that the detection of the flare sign, which is detectable as high-intensity signals around and extending from a metastatic node on fat-suppressed T2-weighted images, provided the best results among the potential MR imaging findings as a diagnostic criterion for ENS; the shaggy margin criterion provided high specificity, but the sensitivity was low. On the other hand, the nodal size was also an important predictor for ENS, but the predictive ability was slightly lower than that of the flare sign and shaggy margin criteria.

ENS is difficult to assess on imaging; for example, King et al[8] used the diagnostic criteria of the presence of indistinct nodal margins, irregular nodal capsular enhancement, and infiltration of the cancers into the adjacent fat or muscle. These criteria may be difficult to judge in some cases, and the detection depends on the reader. In the present study, we evaluated a new criterion that is readily detectable on fat-suppressed T2-weighted images (the flare sign). We found that the reproducibility of judging this MR imaging criterion is good. This may be partly due to the fact that fat signals are effectively suppressed by the SPIR technique. The high-intensity signal on the fat-suppressed T2-weighted images indicates water-rich content outside of the capsule of a node and is a reliable indicator of ENS.

At present, it is not clear what the flare sign in the interstitial tissues indicates. One possible explanation would be that the high-intensity signals around and extending from the ENS-positive node are caused by perinodal lymphedema. An imbalance between lymph formation and absorption into lymphatic vessels can be caused by inflammatory or neoplastic obstruction of the lymphatic vessels and results in edema.[11] Lymph fluid might leak from the ruptured capsules of ENS-positive nodes. These changes caused by ENS-positive nodes may lead to the high signal intensity on fat-suppressed T2-weighted images. The lymph in the interstitial tissues may contain metastatic cancer cells that have infiltrated from the tumor surface in the metastatic nodes and may facilitate dissemination of cancer cells.[11]

The proposed MR imaging criterion (flare sign) yielded high specificity and negative predictive value without significant loss of sensitivity and positive predictive value (Table 3). Therefore, the criteria used in the present study may be useful for the development of a treatment plan. Radiation therapy was reported to improve survival of the patients with ENS compared with the ENS-positive patients who did not receive radiation therapy.[12] In addition, selective neck dissection instead of radical neck dissection could be a choice for patients with ENS-negative metastatic nodes.[13] The higher negative predictive values of the proposed MR imaging criteria for ENS may be an advantage in the approach to the detection of metastatic nodes with extranodal spread because unnecessary irradiation and surgery could be more effectively avoided in patients with negative findings on fat-suppressed T2-weighted images. Yousem et al[5] obtained good results in predicting ENS by using MR imaging (78%–90% accuracy), but they estimated the diagnostic ability of MR imaging compared with a gold standard using CT on the CT-proof basis instead of pathology, suggesting that CT is more accurate than MR imaging. More recently, King et al[8] evaluated MR imaging in detecting ENS by using a small ($n = 17$) cohort and obtained 78% sensitivity, 86% specificity, and 80% accuracy.

We found that the presence of the shaggy margin on gadolinium-enhanced T1-weighted MR images was also predictive of ENS. In contrast, Yousem et al[5] reported that a contrast-enhanced MR imaging study did not improve the accuracy of detecting ENS. Recent improvements in MR imaging resolution may contribute to the present finding that the shaggy margin of the metastatic node is a reproducible MR imaging criterion for ENS. On contrast-enhanced T1-weighted images, some ENS-positive nodes exhibited disrupted nodal rim enhancement, probably representing the capsular and subcapsular nodal structures destroyed by the cancer cells.[8]

Many (23% with the flare sign and 35% with the shaggy margin criteria) of the histologically positive ENS nodes were negative using the MR imaging criteria (Table 1). Comparison of histologic and MR imaging findings showed that most of these false-negative necks had metastatic nodes with small-volume ENS. Even microscopic ENS can significantly affect a patient's prognosis: The 3-year survival rate was reported to be similar for patients with macroscopic and microscopic ENS, and the survival rate was low in these patients compared with those with intranodal metastasis.[14] Those authors also noted that microscopic ENS can occur even in small-volume metastatic lesions in the node. It is plausible that MR imaging cannot detect microscopic ENS that is associated with focal rupture of the nodal capsule and minor extension of cancer cells. No difference was found in survival between patients with ENS with narrow (<2 mm) or broad (≥ 2 mm) extranodal extensions of metastatic lesions.[15] In addition, the same study showed that patients with multiple ENS-positive nodes had the worst prognosis. These findings suggest that all patients with a single ENS-positive node should be carefully surveyed for additional ENS in the neck at histologic examinations after surgical excision.

It is generally believed that a larger metastatic node is more likely to have ENS. Indeed, we found that the ENS-positive metastatic nodes had significantly greater nodal size than those that were ENS-negative (Table 1). King et al[8] reported that ENS occurred in nodes of <10 mm, but we did not find histologically proved ENS in metastatic nodes <10 mm in the short-axis diameter. On the other hand, about one fifth of ENS-negative metastatic nodes had short-axis diameters of >20 mm. Smeele et al[16] reported that 95% of the patients with metastatic nodes whose average nodal size was 57 ± 24 mm

were ENS-positive. Consistent with these findings, multivariate analysis demonstrated that the nodal size was an important and independent predictor. However, we may have overestimated the size of the cutoff point for ENS because we did not examine the serial sections of the whole metastatic nodes for the ENS surveillance; instead, we examined several histology sections obtained from the maximal nodal areas.

In the present study, we did not evaluate whether these MR imaging findings could be used as grades for the prediction of a patient's prognosis; we speculate that the prognosis would be poor if the interstitial tissues are extensively involved (such as the case exhibiting the flare sign) or the deep cervical muscles are involved by the extranodal tumor cells. The answer to this question must await further studies.

Conclusion

We evaluated the 4 potential MR imaging findings (nodal size, vanishing border sign, flare sign, and shaggy margin) as criteria for the diagnosis of ENS in the neck. Of these findings, the flare sign provided the best results, yielding high specificity and a negative predictive value, and moderate sensitivity and a positive predictive value. Although the combined use of these MR imaging criteria did not significantly improve the diagnostic ability with a single use of the flare sign, the use of these MR imaging criteria (nodal size, flare sign, and shaggy margin) would be useful for the effective diagnosis of ENS in the neck. However, substantial fractions of false-negative and -positive cases still existed.

References

1. Kasperts N, Slotman BJ, Leemans CR, et al. **Results of postoperative reirradiation for recurrent or second primary head and neck carcinoma.** *Cancer* 2006;106:1536–47
2. Leemans CR, Tiwari R, Nauta JJ, et al. **Regional lymph node involvement and its significance in the development of distant metastases in head and neck carcinoma.** *Cancer* 1993;71:452–56
3. Myers JN, Greenberg JS, Mo V, et al. **Extracapsular spread: a significant predictor of treatment failure in patients with squamous cell carcinoma of the tongue.** *Cancer* 2001;92:3030–36
4. Wenzel S, Sagowski C. Kehrl W, et al. **The prognostic impact of metastatic pattern of lymph nodes in patients with oral and oropharyngeal squamous cell carcinomas.** *Eur Arch Otorhinolaryngol* 2004;261:270–75
5. Yousem DM, Som PM, Hackney DB, et al. **Central nodal necrosis and extracapsular neoplastic spread in cervical lymph nodes: MR imaging versus CT.** *Radiology* 1992;182:753–59
6. Sumi M, Sakihama N, Sumi T, et al. **Discrimination of metastatic cervical lymph nodes with diffusion-weighted MR imaging in patients with head and neck cancer.** *AJNR Am J Neuroradiol* 2003;24:1627–34
7. Sumi M, Van Cauteren M, Nakamura T. **MR microimaging of benign and malignant nodes in the neck.** *AJR Am J Roentgenol* 2006;186:749–57
8. King AD, Tse GM, Yuen EH, et al. **Comparison of CT and MR imaging for the detection of extranodal neoplastic spread in metastatic neck nodes.** *Eur J Radiol* 2004;52:264–70
9. Som PM, Curtin HD, Mancuso AA. **Imaging-based nodal classification for evaluation of neck metastatic adenopathy.** *AJR Am J Roentgenol* 2000;174:837–44
10. Chikui T, Yonetsu K, Nakamura T. **Multivariate feature analysis of sonographic findings of metastatic cervical lymph nodes: contribution of blood flow features revealed by power Doppler sonography for predicting metastasis.** *AJNR Am J Neuroradiol* 2000;21:561–67
11. Alitalo K, Carmeliet P. **Molecular mechanism of lymphangiogenesis in health and disease.** *Cancer Cell* 2002;1:219–27
12. Clark J, Li W, Smith G, et al. **Outcome of treatment for advanced cervical metastatic squamous cell carcinoma.** *Head Neck* 2005;27:87–94
13. Simenthal AA Jr, Duvvuri U, Johnson JT, et al. **Selective neck dissection in patients with upper aerodigestive tract cancer with clinically positive nodal disease.** *Ann Otol Rhinol Laryngol* 2006;115:846–49
14. Woolgar JA, Rogers SN, Lowe D, et al. **Cervical lymph node metastasis in oral cancer: the importance of even microscopic extracapsular spread.** *Oral Oncol* 2003;39:130–37
15. Greenbers JS, Fowler R, Gomez J, et al. **Extent of extracapsular spread: a critical prognosticator in oral tongue caner.** *Cancer* 2003;97:1464–70
16. Smeele LE, Leemans CR, Reid CBA, et al. **Neck dissection for advanced lymph node metastasis before definitive radiotherapy for primary carcinoma of the head and neck.** *Laryngoscope* 2000;110:1210–14